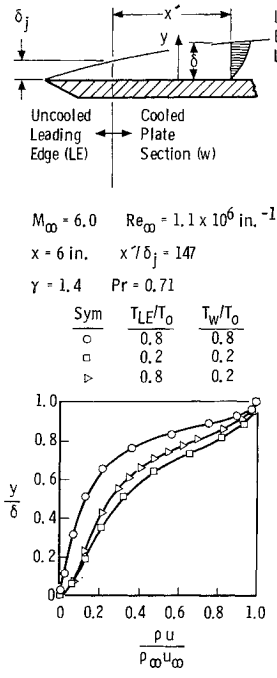

Fig. 2 Theoretical velocity-density product profiles for various model surface temperature distributions.

corresponding to the experimental beginning of transition and show that at $y/\delta = 0.9$, in the region of the critical layer or earliest disturbance-amplifying region, the boundary-layer profile has not adjusted completely to the new wall temperature condition. The percentage of adjustment is related in Fig. 3 to the parameter x'/δ_j, or distance from the leading-edge-to-plate joint divided by the boundary-layer thickness at the joint from Ref. 3. There it is seen that the laminar boundary layer approaching transition has, insofar as the $y/\delta \approx 0.9$ region is concerned, experienced conditions corresponding to considerably higher wall temperatures than existed at the wall. The boundary layer has developed over the two-in. leading edge at hot-wall conditions and then has proceeded to the beginning of transition with an average ($0 \leq x'/\delta_j \leq 147$) outer-region accommodation to the new wall temperature of only 55% and a local value at the beginning of transition ($x'/\delta_j = 147$) of about 67%. A calculation of the reduction of uncooled leading-edge length required for 90% critical layer accommodation to the cold wall conditions, with distance to transition remaining fixed at $x = 6$ in., gives the result that the uncooled length must be reduced from two in. to 0.35 in.

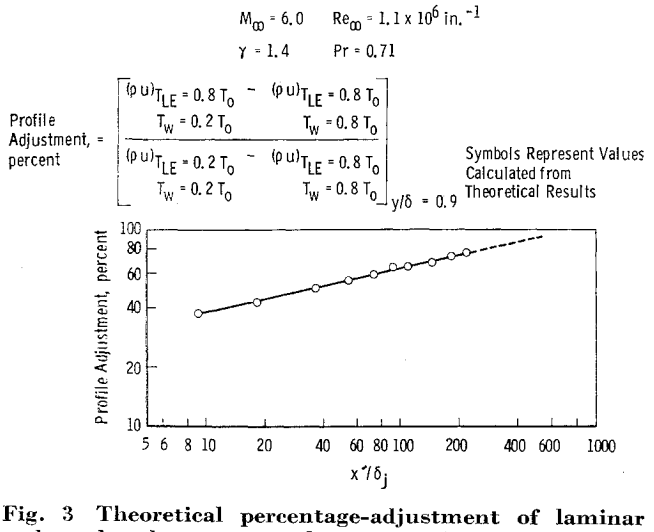

Fig. 3 Theoretical percentage-adjustment of laminar boundary layer to step change in wall temperature.

In conclusion, it appears that for boundary-layer transition experiments examining the effects of wall cooling, a careful consideration of possible hot leading-edge effects is indicated.

References

[1] Richards, B. E. and Stollery, J. L., "Further Experiments on Transition Reversal at Hypersonic Speeds," *AIAA Journal*, Vol. 4, No. 12, Dec. 1966, p. 2224.

[2] Pate, S. R. and Schueler, C. J., "Effects of Radiated Aerodynamic Noise on Model Boundary-Layer Transition in Supersonic and Hypersonic Wind Tunnels," TR-67-236 (AD666644), March 1968, Arnold Engineering Development Center; also AIAA Paper 68-375, San Francisco, Calif. 1968.

[3] Lewis, C. H., private communication, 1968, Virginia Polytechnic Institute, Blacksburg, Va.

[4] Jaffe, N. A., Lind, R. C., and Smith, A. M. O., "Solutions to the Binary Diffusion Laminar Boundary-Layer Equations Including the Effect of Second-Order Transverse Curvature," TR-66-183 (AD647285), Feb. 1967, Arnold Engineering Development Center.

Transient Stresses at a Clamped Support of an Orthotropic, Circular, Cylindrical Shell

M. J. Forrestal* and M. J. Sagartz†
Sandia Laboratories, Albuquerque, N.Mex.

Introduction

MANY composite materials have improved the efficiency of structural elements for aerospace vehicles. Since unlimited types of composite materials are possible, it is imperative to provide analyses which can guide the selection of efficient materials. In this analysis, the transient bending and shear stresses at the clamped support of a semi-infinite, orthotropic, circular, cylindrical shell produced by a uniform, radial impulse are calculated from the shell bending theory and a Timoshenko-type shell theory. These results provide design criteria for the shell requirements in the vicinity of stiff ring supports.

The title problem was recently investigated for an isotropic shell.[1] This Note generalizes the work in Ref. 1 by considering an orthotropic shell.

Shell Equations of Motion

Timoshenko-type equations which govern the axially symmetric motion of orthotropic, circular, cylindrical shells are presented in Ref. 2. The axial normal stress is taken as zero, and the shell equations reduce to

$$\frac{\kappa^2(1-\nu_{x\theta}\nu_{\theta x})G}{E_\theta}\left[\frac{\partial^2 W}{\partial\eta^2}-\frac{\partial\psi}{\partial\eta}\right]-(1-\nu_{x\theta}\nu_{\theta x})W=\frac{\partial^2 W}{\partial\tau^2}-\frac{c(1-\nu_{x\theta}\nu_{\theta x})}{hE_\theta}I\delta(\tau) \quad (1a)$$

$$\frac{h^2}{12a^2}\frac{\partial^2\psi}{\partial\eta^2}+\frac{\kappa^2 G(1-\nu_{x\theta}\nu_{\theta x})}{E_x}\left[\frac{\partial W}{\partial\eta}-\psi\right]=\frac{h^2E_\theta}{12a^2E_x}\frac{\partial^2\psi}{\partial\tau^2} \quad (1b)$$

Received October 1, 1969; revision received October 31, 1969. This work was supported by the U.S. Atomic Energy Commission.

* Staff Member. Member AIAA.
† Staff Member.

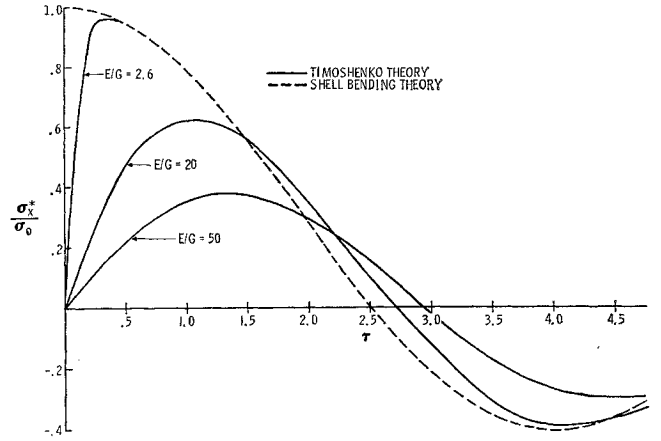

Fig. 1 Bending stress for $a/h = 10$, $\nu = 0.3$.

$$\nu_{x\theta}E_x = \nu_{\theta x}E_\theta \tag{1c}$$

$$W = w/a; \quad \eta = x/a; \quad \tau = ct/a; \quad c^2 = E_\theta/\rho(1 - \nu_{x\theta}\nu_{\theta x}) \tag{1d}$$

where a and h are the shell radius and thickness; E_θ, E_x are Young's moduli; $\nu_{x\theta}$, $\nu_{\theta x}$ are the Poisson's ratios; G is the transverse shear modulus; w is the radial shell displacement, measured positive inward; ψ is the angle of rotation of a normal to the middle surface, measured positive clockwise; x is the axial coordinate; t is time; I is the impulse intensity; and $\delta(\tau)$ is the Dirac delta function. The notation for the material properties is the same as that used in Ref. 3, and the shear deflection coefficient κ^2 which is discussed in Ref. 2 is taken as $\pi^2/12$ for this study.

The magnitude of bending stress at the outer surfaces of the shell $\sigma_x{}^*$ and shear stress resultant Q_x are related to ψ and W by

$$\sigma_x{}^* = [\pm Eh/2a(1 - \nu_{x\theta}\nu_{\theta x})]\partial\psi/\partial\eta \tag{2a}$$

$$Q_x = \kappa^2 Gh(\psi - \partial W/\partial\eta) \tag{2b}$$

Bending Stress at the Clamped Support

A formal solution for the magnitude of bending stress at the outer surface of the shell at the clamped support is obtained by following the procedure outlined in Ref. 1. This leads to the following integral expression for the stress:

$$\sigma_x{}^* = \frac{1}{2\pi i}\int_{-i\infty+b}^{+i\infty+b} \frac{Ic\beta^2}{2a} \cdot \frac{e^{p\tau}dp}{(p^2 + 1 - \nu_{x\theta}\nu_{\theta x})^{1/2}[(p^2 + 1 - \nu_{x\theta}\nu_{\theta x})^{1/2} + \gamma(p^2 + \beta^2)^{1/2}]} \tag{3a}$$

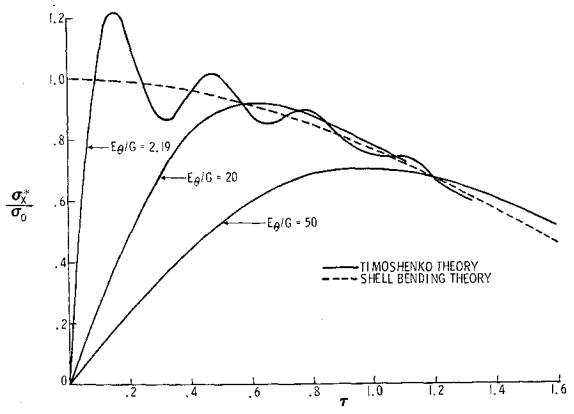

Fig. 2 Bending stress for $a/h = 10$, $E_\theta/E_x = 10$, $\nu_{x\theta} = 0.3$, $\nu_{x\theta} = 0.03$.

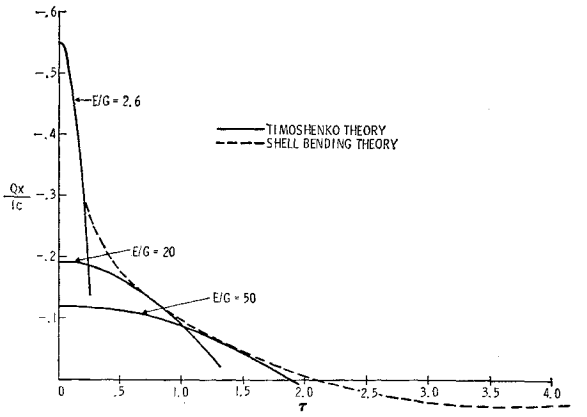

Fig. 3 Shear stress resultant for $a/h = 10$, $\nu = 0.3$.

in which

$$\beta^2 = \frac{12a^2\kappa^2 G(1 - \nu_{x\theta}\nu_{\theta x})}{h^2 E_\theta}; \quad \gamma^2 = \frac{\kappa^2 G(1 - \nu_{x\theta}\nu_{\theta x})}{E_x} \tag{3b}$$

The functional form of Eq. (3a) is the same as the formal solution for the isotropic shell presented in Ref. 1; however, the definitions of β and γ are different. Then the solution is the same as that presented for the isotropic case if the definitions for β and γ given by Eq. (3b) are used. Thus

$$\sigma_x{}^* = \frac{Ic\beta^2\gamma}{\pi a}\int_{(1-\nu_{x\theta}\nu_{\theta x})^{1/2}}^{\beta} \times \frac{[y^2 - (1 - \nu_{x\theta}\nu_{\theta x})]^{1/2}[\beta^2 - y^2]^{1/2}\sin y\tau dy}{[y^2 - (1 - \nu_x\nu_{\theta x})]^2 + \gamma^2[y^2 - (1 - \nu_{x\theta}\nu_{\theta x})][\beta^2 - y^2]} \tag{4}$$

To isolate the effects of rotary inertia and transverse shear deformation, the problem is also analyzed on the basis of the shell bending theory. The shell equation of motion for this theory with the axial normal stress taken as zero is

$$\frac{h^2}{12a^2}\frac{\partial^4 W}{\partial\eta^4} + \frac{(1 - \nu_{x\theta}\nu_{\theta x})E_\theta}{E_x}W + \frac{E_\theta}{E_x}\frac{\partial^2 W}{\partial\tau^2} = \frac{c(1 - \nu_{x\theta}\nu_{\theta x})I}{E_x h}\delta(\tau) \tag{5}$$

and the solution for the bending stress is

$$\sigma_x{}^*/\sigma_0 = J_0[(1 - \nu_{x\theta}\nu_{\theta x})^{1/2}\tau] \tag{6a}$$

where

$$\sigma_0 = (I/h)[3E_x/\rho(1 - \nu_{x\theta}\nu_{\theta x})]^{1/2} \tag{6b}$$

and J_0 is the Bessel function of the first kind of order zero.

Shear Stress Resultant at the Clamped Support

Complete evaluation of the formal integral solution for the shear stress resultant at the support would be extremely cumbersome. However, the early time response can be obtained by power series expansion of the transformed solution using the Timoshenko-type shell theory whereas at later times the shell bending theory is adequate.

The early time response is obtained by expanding the transformed solution in powers of $1/p$ where p is the transform variable. Inversion of the first two nonzero terms gives

$$Q_x = -\gamma Ic\left(\frac{E_x}{E_\theta}\right)^{1/2}\left\{1 - \left[\frac{\gamma^2(\beta^2 + 1 - \nu_{x\theta}\nu_{\theta x} - E_x/\kappa^2 G)}{2(1 + \gamma)^2} + \frac{(1 - \nu_{x\theta}\nu_{\theta x})}{1 + \gamma}\right]\frac{\tau^2}{2} + \ldots\right\} \tag{7}$$

where β and γ were defined in Eq. (3b). The shear stress

resultant predicted by the shell bending theory is

$$Q_x = \frac{-Ic(\pi h/a)^{1/2}}{\Gamma(\frac{1}{4})}\left[\frac{2E_x(1-\nu_{x\theta}\nu_{\theta x})^{1/2}}{3E_\theta\tau}\right]^{1/4} \times J_{-1/4}[(1-\nu_{x\theta}\nu_{\theta x})^{1/2}\tau] \quad (8)$$

where Γ is the gamma function and $J_{-1/4}$ is the Bessel function of the first kind of order $-\frac{1}{4}$. Q_x predicted by the shell bending theory has a singularity of the type $(\tau)^{-1/2}$ as $\tau \to 0$; whereas the Timoshenko-type shell theory predicts a finite value.

Discussion and Numerical Results

In view of Eq. (1c), there are four independent elastic constants for the orthotropic material. For the special case where $E_x = E_\theta = E$ and $\nu_{x\theta} = \nu_{\theta x} = \nu$, there are three independent elastic constants E, ν, G; this material is termed transversely isotropic. The bending stress at the outer surfaces of a shell with $a/h = 10$ predicted by both shell theories for a transversely isotropic material is shown in Fig. 1. The ratio $E/G = 2.6$ corresponds to the isotropic case for $\nu = 0.30$, and the values $E/G = 20$ and 50 correspond to pyrolytic graphite. These results indicate that the shell bending theory becomes less accurate for predicting maximum bending stresses as the E/G ratio increases and that the bending stresses are reduced as G is reduced. Results for an orthotropic material with $E_\theta/E_x = 10$ and $a/h = 10$ are presented in Fig. 2. These results indicate that the bending stresses are reduced as E_x is reduced.

The response of the shear stress resultant at the clamped support for a transversely isotropic material is presented in Fig. 3 for $a/h = 10$. The early time response is described by Eq. (7) and the remainder of the response is described by Eq. (8). Then the entire response can be closely approximated for the entire regime by piecing the two solutions together.

References

[1] Sagartz, M. J. and Forrestal, M. J., "Transient Stresses at a Clamped Support of a Circular Cylindrical Shell," *Journal of Applied Mechanics*, Vol. 36, No. 2, June 1969, pp. 367–369.

[2] Baker, E. H. and Herrmann, G., "Vibrations of Orthotropic Cylindrical Sandwich Shells under Initial Stress," *AIAA Journal*, Vol. 4, No. 6, June 1966, pp. 1063–1070.

[3] Kraus, H., *Thin Elastic Shells*, Wiley, New York, 1967.

Postbuckling Behavior of Geometrically Imperfect Composite Cylindrical Shells under Axial Compression

N. S. Khot*
Air Force Flight Dynamics Laboratory, Wright-Patterson Air Force Base, Ohio

THIS Note is concerned with the influence of initial geometric imperfections on the buckling behavior of laminated anisotropic cylindrical shells. It has been established that the geometric imperfections reduce the buckling strength of isotropic cylindrical shells and the extent of the reduction has been studied intensively.[1,2] A similar reduction in buckling strength due to initial geometric imperfections may be expected in case of the anisotropic shells. In the present analysis von Kármán-Donnell large displacement relations, modified to include geometric imperfections are used. The solution to the problem is obtained by the application of the principle of stationary potential energy.

Presented as Paper 69-93 at the AIAA 7th Aerospace Sciences, Meeting, New York, January 20–22, 1969; submitted February 5, 1969; revision received October 10, 1969.

* Aerospace Engineer, Structures Division. Member AIAA.

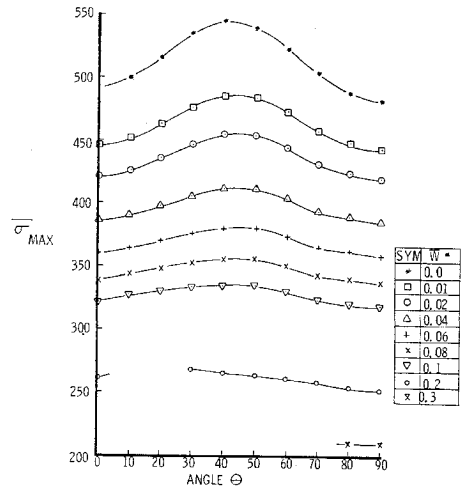

Fig. 1 Influence of initial imperfection on buckling load of three-layer, glass-epoxy composite cylinder for fiber orientation ($\theta°, -\theta°, 0°$).

Analytical Formulation

The relations between resultant stresses and strains for the laminated shell wall can be written as

$$[\epsilon] = [a][N] + [d]^T[k] \quad [M] = [d][N] - [d^*][k] \quad (1)$$

where $[\epsilon]$, $[k]$ represent strains and changes of curvature while $[N]$ and $[M]$ are resultant stresses and moments. The definitions of matrices $[a]$, $[d]$, and $[d^*]$ may be found in Ref. 3.

The total strain energy of a multilayered cylindrical shell of radius R and length L can be expressed as the sum of the following two expressions:

$$\pi_1 = \frac{1}{2}\int_0^L \int_0^{2\pi R} [N]^T[a][N]dxdy$$
$$\pi_2 = \frac{1}{2}\int_0^L \int_0^{2\pi R} [K]^T[d^*][K]dxdy \quad (2)$$

The energy associated with the work done by the uniformly applied compressive end load $\bar{\sigma}$ is given by

$$\pi_3 = L\int_0^{2\pi R}\{-\bar{\sigma}\}\,dy\int_0^L \bar{\varepsilon}dx \quad (3)$$

where $\bar{\varepsilon}$ is the unit end shortening.

The total potential energy is then given by

$$\pi = \pi_1 + \pi_2 + \pi_3 \quad (4)$$

The functions selected to represent the total radial displacement W and the initial imperfection $\bar{W}$ are given below:

$$W = W_1\cos\frac{\pi x}{l_x}\cos\frac{\pi y}{l_y} + W_2\cos\frac{2\pi x}{l_x} + W_3\cos\frac{2\pi x}{l_x}\cos\frac{2\pi y}{l_y} + W_4\cos\frac{4\pi x}{l_x} + W_0 \quad (5)$$

$$\bar{W} = \bar{W}_1\cos\frac{\pi x}{l_x}\cos\frac{\pi y}{l_y} + \bar{W}_2\cos\frac{2\pi x}{l_x} + \bar{W}_3\cos\frac{2\pi x}{l_x}\cos\frac{2\pi y}{l_y} + \bar{W}_4\cos\frac{4\pi x}{l_x}$$

where W_0 through W_4 are the unknown coefficients and $\bar{W}_1$